Available online at www.sciencedirect.com
SCIENCE DIRECT
Journal of Power Sources 154 (2006) 192–197
JOURNAL OF POWER SOURCES
www.elsevier.com/locate/jpowsour

Short communication

Modelling fuel cell performance using artificial intelligence

S.O.T. Ogaji *, R. Singh, P. Pilidis, M. Diacakis

Power Propulsion and Aerospace Engineering Department, Centre for Diagnostics and Life Cycle Costs, Cranfield University, UK

Received 16 August 2004; received in revised form 5 February 2005; accepted 14 March 2005
Available online 23 June 2005

Abstract

Over the last few years, fuel cell technology has been increasing promisingly its share in the generation of stationary power. Numerous pilot projects are operating worldwide, continuously increasing the amount of operating hours either as stand-alone devices or as part of gas turbine combined cycles. An essential tool for the adequate and dynamic analysis of such systems is a software model that enables the user to assess a large number of alternative options in the least possible time. On the other hand, the sphere of application of artificial neural networks has widened covering such endeavours of life such as medicine, finance and unsurprisingly engineering (diagnostics of faults in machines). Artificial neural networks have been described as diagrammatic representation of a mathematical equation that receives values (inputs) and gives out results (outputs). Artificial neural networks systems have the capacity to recognise and associate patterns and because of their inherent design features, they can be applied to linear and non-linear problem domains. In this paper, the performance of the fuel cell is modelled using artificial neural networks. The inputs to the network are variables that are critical to the performance of the fuel cell while the outputs are the result of changes in any one or all of the fuel cell design variables, on its performance. Critical parameters for the cell include the geometrical configuration as well as the operating conditions. For the neural network, various network design parameters such as the network size, training algorithm, activation functions and their causes on the effectiveness of the performance modelling are discussed. Results from the analysis as well as the limitations of the approach are presented and discussed.

Keywords: Neural network; Artificial intelligence; Fuel cell

1. Introduction

Ever since the birth of the power generation industry there has been a need for efficient and clean generation of electrical energy that can cope with the increase of power demand, and the adverse forecasts of fuel supplies. Fuel cell technology has proven to be a technology capable of assisting such an effort [1,2] either as a stand-alone technology [3] or by combining with Turbomachinery equipment [4,5]. Their cost may still be prohibitive and a hydrogen production infrastructure in its infancy but their inherent advantages, such as low emissions and very high conversion efficiencies, as well as the low maintenance requirements due to the absence of moving or rotating parts make them an attractive possibility.

On the other hand,, the sphere of application of ANN has grown covering such endeavours of life as medicine, finance and engineering amongst others. In engineering, areas of application includes single sensor fault identification in industrial power plants [6], diagnosis of sensor and component faults in gas turbines [7], signal validation, control and diagnostics in nuclear power plants [8], mechanical rotor system unbalance [9] and a machine tool monitoring in metal cutting processes [10]. Recently [11], the application of ANN in predicting the stack voltage of a proton exchange membrane fuel cell (PEMFC) was considered. In their analysis, four parameters namely stack current, stack temperature, hydrogen and oxygen flow were used as input to the network with the stack voltage being the only output.

Essential for the proper evaluation of fuel cell technology and simulation processes, in general, are performance models, which will allow for the investigation of the operating characteristics either on a stand alone basis or as part of

* Corresponding author. Tel.: +44 1235 750 111; fax: +44 1234 751 232.
E-mail address: s.ogaji@cranfield.ac.uk (S.O.T. Ogaji).

0378-7753/$ – see front matter © 2005 Elsevier B.V. All rights reserved.
doi:10.1016/j.jpowsour.2005.03.226

Nomenclature

A	area (m^2)
ANN	artificial neural network
F	Faraday's constant ($C\,mole^{-1}$)
ΔG	Gibbs free energy
ΔH	enthalpy change
HL	hidden layer
I	current density ($A\,m^{-2}$)
IL	input layer
l	length (m)
LHV	lower heating value ($kJ\,mole^{-1}$)
m	mass flow rate ($moles\,s^{-1}$)
MSE	mean square error
n	number of electrons
OL	output layer
$\overline{p}$	partial pressure (bar)
P	pressure (bar)
r	universal gas constant ($J\,kmole^{-1}$)
R	air ratio (%)
R_{anode}	anode activation polarisations
$R_{cathode}$	cathode activation polarisations
ΔS	entropy change
SOFC	solid oxide fuel cell
T	cell temperature (K)
U_f	fuel utilisation (%)
U_o	air utilisation (%)
V_G	Gibbs cell potential (V)
V_{cell}	deliverable cell potential (V)
W	cell power (W)

Subscripts

a	anode
c	cathode
el	electrolyte
G	Gibbs
N	Nernst

Greek letters

η	cell thermal efficiency (%)
σ	standard deviation

cycle where other components will be involved. Further with computational time being one of the major issues in simulation efforts, artificial intelligence can be implemented in order to reduce assessment period.

2. Fundamentals

2.1. Solid oxide fuel cells

A fuel cell is a device that converts the chemical energy of hydrogen or hydrogen containing fuel, such as a hydrocarbon, alcohol or other, to electricity by means of an electrochemical reaction. A major distinction between fuel cells and other devices delivering electricity, such as heat engines, is that only a single energy conversion step is needed. That is, the chemical energy is converted directly to electricity with heat produced only as a by-product. The main components of a cell, as shown in Fig. 1, are the two electrodes, each covered with a thin layer of a catalyst, and the electrolyte positioned in between them. Fuel is supplied to the anode electrode, while oxygen or air is fed to the cathode electrode. The electrolyte serves the function of isolating electronically the electrodes anode and forming an ionic bridge between them.

The material commonly used for the electrolyte is zirconia dioxide (ZrO_2), doped with 8–10 mole% yttria trioxide (Y_2O_3). The final name of the electrolyte is yttria stabilised zirconia (YSZ). The anode material is Ni showing high electrochemical activity for the hydrogen oxidation reaction. To Ni a composite material similar to the one used for the electrolyte, i.e. yttria stabilised zirconia is added in order to adjust the thermal expansion coefficient of the anode and the electrolyte with the final product called Ni–yttria stabilised zirconia cermet. Finally cathodes, material is based on the perovskites lanthanum manganite with the La being replace with by strontium yielding strontium (Sr) doped lanthanum (La) manganite (Mn), i.e. $LaSrMnO_3$.

During operation, oxygen atoms interact with the catalyst on the cathode electrode and as a consequence oxygen ions are formed and travel through the electrolyte towards the anode. There they react with the hydrogen that has been produced by the reforming and water shift reaction of methane, and form water. The electrons released from the hydrogen atoms reach the cathode by means of an external electrical connection, i.e. the load. The operating temperature is in the vicinity of 1000 °C. Clearly, the operation of fuel cells resembles the operation of a battery with the difference being that in a battery the amount of electricity generated is limited by the quantity of reagents stored in it while in fuel cells electricity is continuously produced as long as oxygen and fuel are fed to the electrodes.

The three physical processes that occur during the cell operation are described with the following equations, namely

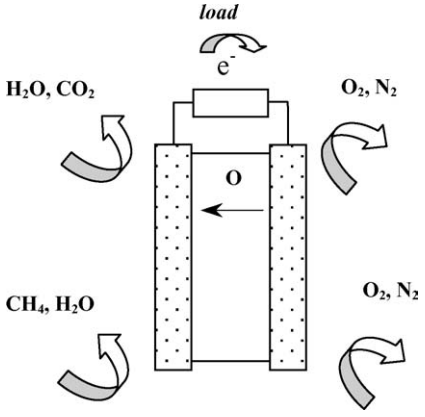

Fig. 1. SOFC schematic.

the reforming process, the water shift reaction and the combustion of hydrogen.

$$CH_4 + H_2O \rightarrow CO + 3H_2 \quad (1)$$

$$CO + H_2O \rightarrow CO_2 + H_2 \quad (2)$$

$$H_2 + 0.5O_2 \rightarrow H_2O \quad (3)$$

Since the analysis is taking place under isobaric conditions the Gibbs free energy expresses the theoretical maximum available energy in the process.

$$\Delta G = \Delta H - T\Delta S \quad (4)$$

And so the theoretical maximum potential can be derived.

$$V_G = -\frac{\Delta G}{nF} \quad (5)$$

where F is the Faraday's constant (=96,486 C mole^{-1}) and n is the number of electrons involved in the process, two for the case of a SOFC.

Further, the open cell potential (V_{cell}) or otherwise called Nernst voltage (V_N) has to be computed in order to take into account the effect of pressure and temperature

$$V_N = V_G - \frac{RT}{nF} \ln\left(\frac{\overline{p_{H_2O}}}{\overline{p_{H_2}}\sqrt{\overline{p_{O_2}}}}\right). \quad (6)$$

In the same way, heat engines never reach their maximum theoretical efficiency due to irreversibilities so do fuel cells as a consequence of internal resistances called polarisation effects which come principally in two main groups: activation and Ohmic.

During operation, in the region next to the electrodes an electric field is formed which influences the motion of the ions. Electrochemical reactions involve barriers, which must be overcome by the reacting species. This energy barrier is called activation energy and results in polarisation, which is due to the transfer of charges between the electronic and the ionic conductors. The activation polarisation may be regarded as the extra potential necessary to overcome the energy barrier of the rate-determining step of the reaction. For fast reaction rates and small currents, activation polarisations are relatively insignificant but as the rate of reaction slows down and the current increases they tend to increase. Anode and cathode activation polarisation is given by the following formulas:

$$\frac{1}{R_{anode}} = K_{anode}\frac{2F}{RT}\left(\frac{\overline{p_{H_2}}}{p}\right)^{0.25} e^{-E_{anode}/RT} \quad (7)$$

$$\frac{1}{R_{cathode}} = K_{cathode}\frac{4F}{RT}\left(\frac{\overline{p_{O_2}}}{p}\right)^{0.25} e^{-E_{cathode}/RT} \quad (8)$$

Like all conducting materials, the electrodes and the electrolyte of cell posses an electric resistance either to electrons or to ions yielding to Ohmic polarisations, which tend to increase as the current increases. Ohmic resistance is obtained by use of the following correlation:

$$R_{component} = l_{component}A_{component}\, e^{-B_{component}/T} \quad (9)$$

The final voltage delivered by the cell is a function of three parameters, the maximum theoretical voltage, the open cell voltage and the polarisation losses

$$V_{cell} = V_N - I(R_{activation} + R_{Ohmic}) \quad (10)$$

The power output of the cell is expressed as a function of operating current density and voltage

$$P_{cell} = IV_{cell}A \quad (11)$$

Finally, the efficiency is defined as the desired output, i.e. power over the required input, i.e. fuel flow:

$$\eta_{th} = \frac{P_{cell}}{m\,LHV} \quad (12)$$

2.2. Artificial neural networks

Neurobiology estimates the human brain to consist of 100 billion nerve cells or neurons [12]. Biological neurons have three principal components: the dendrites, the cell body and the axon. On the other hand, a typical artificial neuronal model is comprised of weighted connectors, an adder and a transfer function (Fig. 2).

The basic relationship as displayed by this neuronal model is:

$$n = wp + b \quad (13)$$

$$a = F(wp + b) = F(n) \quad (14)$$

where a is network output signal, w weight of output signal, p input signal, b neuron specific bias, F transfer/activation function, n induced local field or activation potential

From Eqs. (13) and (14), it can be seen that a simple neuron performs the linear sum of the product of the synaptic weight and input with the bias which value is then passed through activation or transfer function that limits the amplitude of the output of a neuron. Activation functions can take various forms ranging from hard limit, through pure linear to sigmoid and the choice of which to use depends on the desired output from the network. Two key similarities between biological and artificial networks [13] are the fact

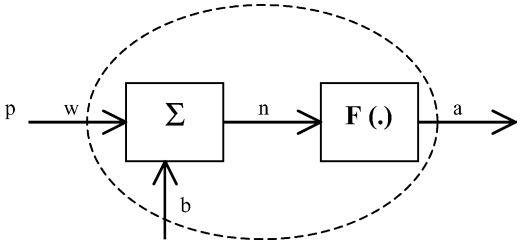

Fig. 2. A single neuronal model.

that their building blocks are highly interconnected computational devices though the artificial neurons are inferior to their biological counterparts and also that the function of the network is determined by the nature of connection between the neurons.

Three fundamental network architectures are popular, viz. single-layer feedforward networks, multi-layer feedforward networks and recurrent networks. The single layered networks have very limited uses while recurrent networks are popular with control systems. However, multi-layered networks have been used in various applications including those mentioned earlier. In this paper, the networks are defined according to the number of layers (including the input parameter layer) with the number of neurons in each layer. Thus, a multi-layered feedforward network defined as 7-5-5-4 implies seven input parameters; five neurons in the first layer; five neurons in the second layer and four neurons in the third layer (which also indicates the number of parameters whose values are being modelled).

The steps involved in obtaining an appropriate back propagation feedforward network (BPNN) as an instance are:

- *Assess the problem* to be solved in a bid to seek the possibility of discretising it.
- *Generate training and test data*. Input and output delta variables used in training and testing the networks could be computed from:

$$\Delta Z = \frac{Z - Z_{\text{estbaseline}}}{Z_{\text{estbaseline}}} \times 100 \tag{15}$$

where $Z_{\text{estbaseline}}$ is the established baseline condition and Z is the measured or calculated value. Network input and output data based on deviation from a common baseline allow for equal representation of all parameters in determining connection weights especially in cases where the magnitudes of these parameters vary widely from one another.

- *Training the network*. The training process juggles the weights and biases to obtain the set that optimises performance via reduced errors and good generalisation. The weight adjustment (noting that BPNN operates on the gradient descent technique) is done via the relation:

$$\Delta w_{ij}(k) = \beta\left(-\frac{\partial E(k)}{\partial w_{ij}}\right) + \alpha \Delta w_{ij}(k-1) \tag{16}$$

where E is the difference between the outputs and the targets for the kth input otherwise called the "error" to be minimised, w the connection weight, β and α are the learning rate and momentum constants, respectively.

3. Methodology

For the purposes of the study, a simulation model in Fortran 90, based on the open literature [14,15] was used to analyse the performance of a SOFC, with the following assumptions taken into consideration.

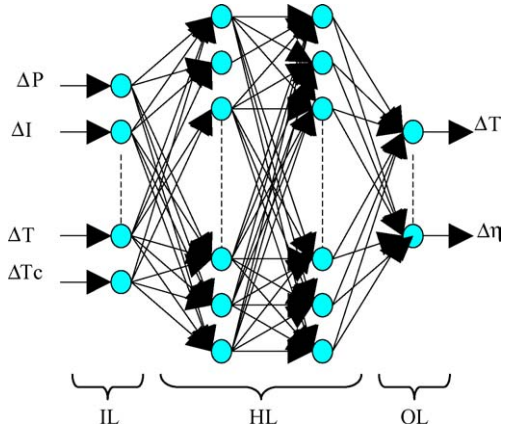

Fig. 3. A two-hidden layered feedforward network.

- Steady-state conditions;
- all three reactions, i.e. reforming of methane, water gas shift and hydrogen electrochemical combustion reach equilibrium;
- the electrochemical oxidation of carbon monoxide was not favoured in the operating temperature to the degree the shift reaction did;
- cell operated under adiabatic conditions;
- anode and cathode exit temperature are equal to the cell operating temperature;
- pressure losses are taken as fixed with a drop equal to 5% of inlet pressure.

The model carries out a thermo-electrochemical analysis of the cell where the power output is computed along with the enthalpy change between inlet and outlet. Results are fed into the energy balance equation and with the help of the secant method convergence is reached and the final operating point is found.

On the other hand, the ANN model used in simulating the performance of the SOFC is akin to that shown in Fig. 3. Seven input and four output variables shown in Table 1 were considered. Scaled conjugate training algorithm was used and a sigmoid transfer function (hyperbolic tangent) used on all layers. With prior knowledge of the number of input and

Table 1
Network I/O parameters and ranges

	Range considered	Baseline
Input		
P (bar)	1–5	1
I (A m^{-2})	500–8000	3000
U_f (%)	0.83–0.87	0.85
U_o (%)	0.24–0.28	0.26
T_a (K)	700–900	900
T_c (K)	700–900	900
Output		
T (K)		1209.65
V (V)		0.5889
W (W)		17.67
η (%)		47.971

Table 2
Electrochemical coefficients

A_a (Ω cm)	0.00298
A_{el} (Ω cm)	0.00294
A_c (Ω cm)	0.008114
B_a (K)	1392
B_{el} (K)	−10350
B_c (K)	−600
K_a (A cm^{-2})	2.13E4
K_c (A cm^{-2})	1.49E4
E_a (kJ mole^{-1})	110
E_c (kJ mole^{-1})	160

output variables, the number of neurons in the IL and OL are defined, thus the optimal network was obtained by varying the number of neurons in the HL.

Table 1 presents the range of the input parameters used to evaluate the performance of a solid oxide fuel cell and to train the artificial neural network.

Furthermore, the values for the various coefficients are presented in Table 2.

4. Results and discussion

Four parameters were of primary interest in the performance of the cell, namely the operating voltage of the cell, the operating efficiency, the power output and the temperature generated. The graphs (Figs. 4–7) present results from the analysis carried out with the simulation code and the trained neural network. It can be seen that overall the discrepancies are negligible and only on certain occasions can one distinguish between the two approaches.

For the first parameter, i.e. voltage it has been observed that as more current is drawn from the cell as less potential is delivered until eventually it collapses. The critical point, not shown in Fig. 4, lies at around 11,000 A m^{-2} where the voltage falls to 0.3 V. As previously mentioned, the performance of the cell resembles the operation of a battery and the similarity in the trend is similar.

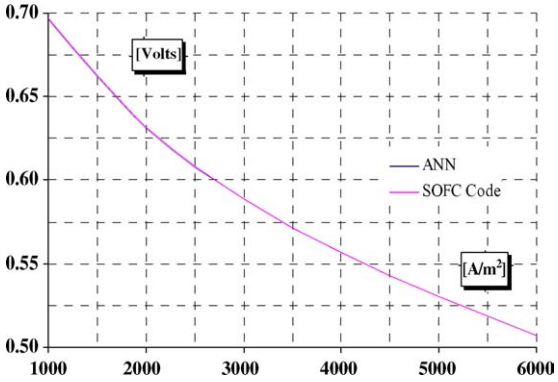

Fig. 4. Voltage vs. current.

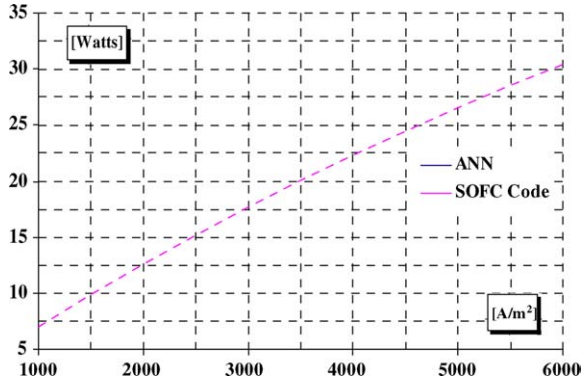

Fig. 5. Power vs. current.

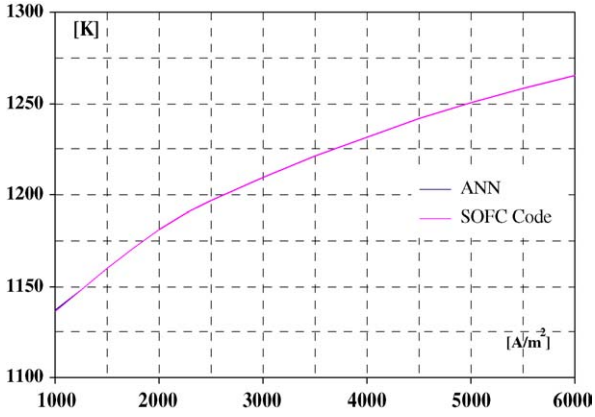

Fig. 6. Temperature vs. current.

The next parameter was cell power. It is obvious from Eq. (11) and the graph that the more current is drawn, for a constant cell area and even though the voltage is decreasing, the power is increasing.

Then the operating temperature was looked at showing an increasing trend as more current is drawn. This is due to the fact that more fuel is fed to the cell and as a result the fraction of energy not converted into electrical work increases the operating temperature.

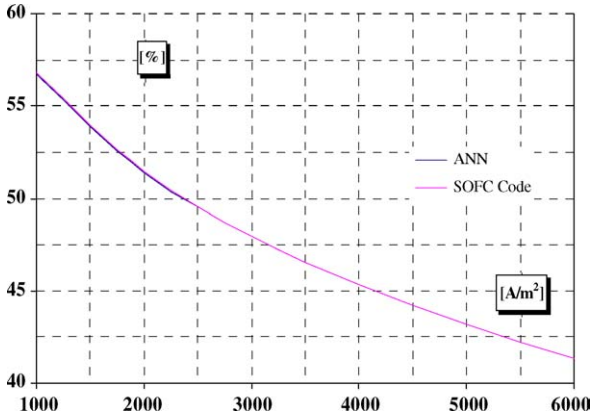

Fig. 7. Efficiency vs. current.

Table 3
Training/test network performance

Architecture	Training MSE	σ error from prediction			
		T	V	W	η
7-5-5-4	8.2×10^{-6}	0.03	0.66	0.65	0.55
7-10-10-4	1.3×10^{-6}	0.01	0.22	0.22	0.22
7-30-30-4	8.6×10^{-7}	0.01	0.16	0.18	0.17

The final parameter of interest was efficiency. The inversely proportional relationship that is shown in the graph, relative to current density is due to the fact that at higher currents there is an increase in the cell polarisation losses.

On a neural network basis a comment that should be made is that of the number of possibilities considered, the performance of three network architectures, the first two randomly selected, are shown in Table 3.

The performance of a network is not only dependent on the mean square error (MSE) achieved during training but also on the networks ability to generalise (apply knowledge gained during training) from data, it has previously not been exposed to. Thus with the σ (standard deviation) values obtained during prediction of the output parameters, the 7-30-30-4 network architecture provided sufficiently accurate results for the intended purpose and was thus adopted. It should be noted that the results reported for the ANN were obtained from tests under different operating conditions but within the range reported in Table 1.

One question that could be stirred up from this research is: *why use ANN when the SOFC algorithm performs creditably*. In addressing this we note that firstly, there could arise scenarios where physical relationship between parameters are not perfectly known, secondly the speed of data processing especially for a large number of cases may be an issue. In these respect amongst others, the verification of the applicability of ANN in SOFC modelling domain is useful especially as ANN has the intrinsic capability to develop parameter relationships where these are not explicitly known, also speed of convergences under different operating points, defined within the set of training data, are high. This goes to support the need for a preliminary trial involving ANN in fuel cell parameter modelling.

5. Conclusions

It has been demonstrated that both traditional computation methods and novel approaches based on artificial intelligence techniques can provide similar accuracy in the modelling of a SOFC. However, further points that can be deduced from this research are:

- The model constructed to simulate the performance of the solid oxide fuel cell shows good accuracy with previous efforts [15].
- Fuel cell technology shows very good performance characteristics, in particular with respect to efficiency, and can help in the general effort for better power generation.
- Artificial intelligence and specifically artificial neural networks can be trained to simulate the performance of a cell with great accuracy; consequently, the same concept could be extended to other components and thus bigger and more complex cycles can be simulated at reduced time.
- ANN is currently applied in various fields such as medicine, predictive regimes and engineering diagnostics. Though the time to set up an ANN system may be long, we, nonetheless, recommend that potential benefit accruable from its incorporation into fuel cell modelling and analysis be further explored.

References

[1] C.G. Vayenas, P.G. Debenedetti, I. Yentekakis, L. Hegedus, Cross-flow, solid-state electrochemical reactors: a steady state analysis, Ind. Eng. Chem. 24 (3) (1985) 316–324.
[2] E. Achenbach, Three-dimensional and time dependent simulation of a planar solid oxide fuel cell stack, J. Power Sources 49 (1994) 333–348.
[3] P. Costamagna, K. Honegger, Modeling of solid oxide heat exchanger integrated stacks and simulation at high fuel utilization, J. Electrochem. Soc. 145 (11) (1998) 3995–4007.
[4] A.F. Massardo, F. Lubelli, Internal reforming solid oxide fuel cell–gas turbine combined cycles (IRSOFC-GT). Part A: cell model and cycle thermodynamic analysis, in: International Gas Turbines and Aeroengine Congress and Exhibition, Stockholm, Sweden, 1998.
[5] S.P. Harvey, H.J. Richter, Gas turbine cycles with solid oxide fuel cells. Part II: a detailed study of a gas turbine cycle with an integrated internal reforming solid oxide fuel cell, J. Energy Resour. Technol. 116 (1994) 312–318.
[6] S. Simani, C. Fantuzzi, Fault diagnosis in power plant using neural networks, Inform. Sci. 127 (2000) 125–136.
[7] S.O.T. Ogaji, R. Singh, Gas path fault diagnoses framework for a 3-shaft gas turbine, ImechE J. Power Energy 217 (A3) (2003) 149–157.
[8] Z. Guo, R.E. Uhrig, Use of artificial neural networks to analyze nuclear power plant performance, Nucl. Technol. 99 (1992) 36–42.
[9] H. Huang, J. Vian, J. Choi, D. Carlson, D. Wunsch, Neural network inverse models for propulsion vibration diagnostics, Proc. SPIE 4390 (1994) 12–21.
[10] M.A. Javed, A.D. Hope, G. Littlefair, D. Adradi, G.T. Smith, B.K.N. Rao, On-line tool condition monitoring using artificial neural networks, Insight 38 (No. 5) (1996) 351–354.
[11] S. Jemei, D. Hissel, M.C. Pera, J.M. Kauffmann, On-board fuel cell power supply modelling on the basis of neural network methodology, J. Power Sources 124 (2003) 479–486.
[12] G. Kevin, An Introduction to Neural Networks, UCL Press Limited, 1997.
[13] S. Haykin, Neural Networks: A Comprehensive Foundation, Prentice Hall, 1999.
[14] U.G. Bossel, Final Report on SOFC data, Facts and Figures, Berne, 1992.
[15] P. Costamagna, L. Magistri, A.F. Massardo, Design and part load performance of a hybrid system based on a solid oxide fuel cell reactor and a micro gas turbine, J. Power Sources 96 (2001) 352–368.